JACS
JOURNAL OF THE AMERICAN CHEMICAL SOCIETY
Article
pubs.acs.org/JACS

Mechanistic Investigations of Water Oxidation by a Molecular Cobalt Oxide Analogue: Evidence for a Highly Oxidized Intermediate and Exclusive Terminal Oxo Participation

Andy I. Nguyen,[†,‡] Micah S. Ziegler,[†] Pascual Oña-Burgos,[§] Manuel Sturzbecher-Hohne,[‡] Wooyul Kim,[∥] Donatela E. Bellone,[†] and T. Don Tilley*[,†,‡]

[†]Department of Chemistry, University of California at Berkeley, Berkeley, California 94720-1460, United States
[‡]Chemical Sciences Division, Lawrence Berkeley National Laboratory, Berkeley, California 94720, United States
[§]Department of Chemistry and Physics, University of Almería, Carretera de Sacramento s/n, 04120 Almería, Spain
[∥]Physical Biosciences Division, Lawrence Berkeley National Laboratory, Berkeley, California 94720, United States

Supporting Information

ABSTRACT: Artificial photosynthesis (AP) promises to replace society's dependence on fossil energy resources via conversion of sunlight into sustainable, carbon-neutral fuels. However, large-scale AP implementation remains impeded by a dearth of cheap, efficient catalysts for the oxygen evolution reaction (OER). Cobalt oxide materials can catalyze the OER and are potentially scalable due to the abundance of cobalt in the Earth's crust; unfortunately, the activity of these materials is insufficient for practical AP implementation. Attempts to improve cobalt oxide's activity have been stymied by limited mechanistic understanding that stems from the inherent difficulty of characterizing structure and reactivity at surfaces of heterogeneous materials. While previous studies on cobalt oxide revealed the intermediacy of the unusual Co(IV) oxidation state, much remains unknown, including whether bridging or terminal oxo ligands form O_2 and what the relevant oxidation states are. We have addressed these issues by employing a homogeneous model for cobalt oxide, the $[Co(III)_4]$ cubane $(Co_4O_4(OAc)_4py_4$, py = pyridine, OAc = acetate), that can be oxidized to the $[Co(IV)Co(III)_3]$ state. Upon addition of 1 equiv of sodium hydroxide, the $[Co(III)_4]$ cubane is regenerated with stoichiometric formation of O_2. Oxygen isotopic labeling experiments demonstrate that the cubane core remains intact during this stoichiometric OER, implying that terminal oxo ligands are responsible for forming O_2. The OER is also examined with stopped-flow UV−visible spectroscopy, and its kinetic behavior is modeled, to surprisingly reveal that O_2 formation requires disproportionation of the $[Co(IV)Co(III)_3]$ state to generate an even higher oxidation state, formally $[Co(V)Co(III)_3]$ or $[Co(IV)_2Co(III)_2]$. The mechanistic understanding provided by these results should accelerate the development of OER catalysts leading to increasingly efficient AP systems.

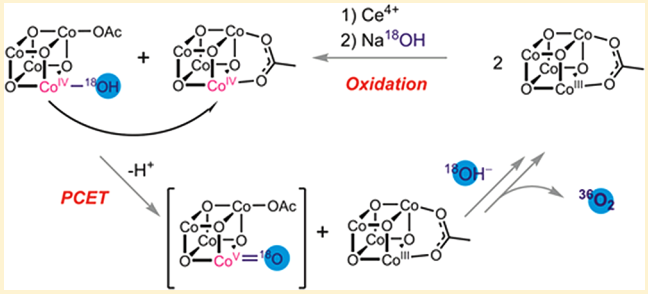

INTRODUCTION

Society's current and future energy demands require sustainable resources that do not contribute to global climate change.[1] While the sun provides abundant energy, conversion of solar energy into a storable, transportable, easily accessible form is not yet economically feasible.[2,3] An ideal system would artificially replicate natural photosynthesis, which involves the endergonic four-electron oxidation of water to O_2 and four protons (eq 1), and the subsequent storage of captured solar

$$2H_2O \rightarrow 4H^+ + 4e^- + O_2 \quad (1)$$

energy in the chemical bonds of a fuel.[4] However, without a catalyst this transformation is inefficient; therefore, research on solar fuel production has focused heavily on the discovery of increasingly efficient water oxidation catalysts (WOCs).[5−8] Mechanistic details of this catalysis, including that of the natural process in photosystem II, is limited but expected to provide important design principles that will enable optimization of catalyst efficiency.[9,10] Much of the mystery associated with such mechanisms concerns the O−O bond-forming event, although several possibilities seem plausible.[8,11]

Cobalt oxide materials are among the most promising catalysts for water oxidation, due to their robust structures, inherent activity, and most importantly, the natural abundance of cobalt.[13−16] Unfortunately, thorough structural characterizations and mechanistic studies of the active species for cobalt oxide catalysts are inherently difficult, given their heteroge-

Received: May 3, 2015
Revised: August 8, 2015
Published: September 21, 2015

DOI: 10.1021/jacs.5b08396
J. Am. Chem. Soc. 2015, 137, 12865−12872

neous nature.[17,18] For heterogeneous catalysts like this, information about the structure and reactivity of the active site can be gained by studying appropriately designed, molecular models. However, while a few soluble, molecular cobalt compounds are reported to behave as active WOCs under photochemical or electrochemical conditions, their associated mechanisms remain poorly defined.[8,19−21] Such investigations are complicated by the difficulty in establishing the integrity of molecular cobalt catalysts under operating conditions, as these compounds may simply serve as precursors to a heterogeneous cobalt oxide catalyst.[22,23] Thus, to date the mechanisms available to soluble and insoluble cobalt-based WOCs are not well understood.

Herein, we provide experimental evidence for the mechanism of water oxidation as catalyzed by a molecular cobalt oxide cluster. This cluster, $Co_4O_4(OAc)_4py_4$ (**1**), was first synthesized in 1998 by Beattie et al., and is an attractive model compound due to its resemblance to a subunit of extended cobalt oxides (Figure 1).[24] The Nocera and Britt groups have employed **1** as

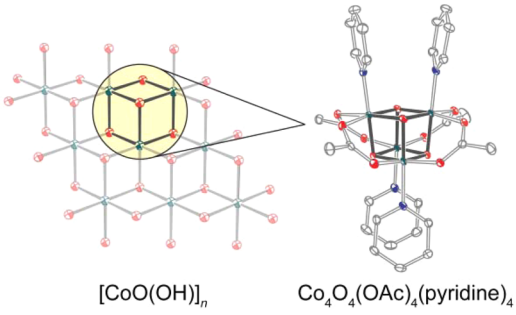

Figure 1. Structural comparison of cobalt oxyhydroxide (CoOOH)[12] with cobalt cubane (**1**). Red, green, blue, and gray spheres or ellipsoids represent O, Co, N, and C, respectively.

a model for the cobalt phosphate (CoP_i) WOC in electron paramagnetic resonance spectroscopy studies.[25] Its promise as a functional model for water oxidation catalysis has been examined by the groups of Dismukes, Scandola, Sun, and Nocera.[26−29] In support of **1** as a possible WOC candidate, density functional theory (DFT) calculations by Siegbahn and co-workers demonstrated the existence of an energetically feasible pathway for O−O bond formation by **1** via a Co(V) intermediate, but their results do not have experimental support.[30] Similarly, theoretical calculations on other cobalt systems suggest that Co(V) is likely the true active intermediate, although the lack of experimental evidence for such species renders it controversial.[31−33] The investigations described below involve a combination of electrochemistry, stoichiometric reactivity, spectroscopy, and kinetic experiments to observe and identify many key intermediates and reaction steps of catalyzed water oxidation involving **1**. In particular, the conversion of hydroxide to oxygen is shown to occur at a molecular $[Co_4O_4]$ cubane center, and the O−O bond formation is demonstrated via a clean stoichiometric reaction from an isolated Co(IV) intermediate. Kinetic studies reveal an unusual mechanism implicating formation of a formal $[Co(III)_3Co(V)]$ or $[Co(III)_2Co(IV)_2]$ intermediate prior to O_2 release. To our knowledge, this is the first example of an isolated WOC intermediate shown to cleanly form O_2 in the absence of exogenous oxidant. Taken together, these data form a clearer picture of how water oxidation is mediated by **1**, and also gives broader implications of how cobalt oxide materials may mediate water oxidation. These should provide a basis for the rational design of more efficient and robust cobalt-based catalysts.

■ ELECTROCHEMISTRY AND REACTION CHEMISTRY

Cubane complex **1** was purified by column chromatography to remove impurities from the crude product obtained using the published synthesis.[29,34] In addition, compound **1** was treated with tetrasodium diaminoethanetetracarboxylate (Na_4EDTA) in the workup to remove any trace Co(II) impurities. To more thoroughly investigate the stability and chemistry of cubane **1** in aqueous solution, cyclic voltammetry (CV) was performed over the pH range from 0.0 to 12. From pH 4 to 10, a 1 mM solution of **1** displays a fully reversible redox couple at $E_{1/2}$ = 1.25 V (vs NHE), corresponding to a one-electron $[Co(III)_4]/[Co(III)_3Co(IV)]$ redox couple ($\mathbf{1}/\mathbf{1}^+$) (Figure 2A). In

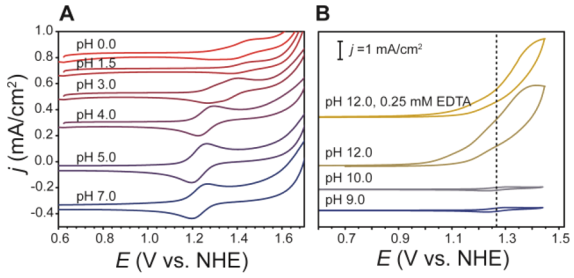

Figure 2. Cyclic voltammograms (100 mV/s) of 1 mM **1** in H_2O with 0.1 M Na_2SO_4 electrolyte at (A) pH 0.0−7.0 and (B) pH 9.0−12.0. The vertical dashed line in panel B shows the $\mathbf{1}/\mathbf{1}^+$ redox couple.

agreement with the results of Nocera and co-workers, purified **1** does not exhibit noticeable catalysis over this pH range, indicating that these samples do not contain Co(II) impurities.[29] This reversible couple shifts linearly with pH to more oxidizing potentials below pH 4, at a rate (63 mV/pH unit) that indicates a $1H^+$, $1e^-$ redox process (Figure S2). The peak potential remains constant below pH 0.7 (to 0), and this behavior is consistent with protonation of cubane **1** to $\mathbf{1}H^+$, with pK_a = 3.5 for **1**. For comparison, the dicationic cobalt cubane complex $[Co_4O_4(OAc)_2(bipy)_4]^{2+}$ exhibits similar behavior, with pK_a = 3.15.[35]

Increasing the pH to 12 results in a significant rise in current density for the anodic wave and bubble formation that is consistent with the catalytic oxidation of hydroxide to oxygen (Figure 2B). By ^1H NMR spectroscopy, a solution of **1** (10 mM in D_2O) at pD 12 shows partial conversion to a new species (*vide infra*), but the total integration of all cobalt species decreased by only 0.9% after 2.5 h, implying that there is only minor decomposition into insoluble or paramagnetic compounds (Figure S3). This electrocatalysis corresponds to an overpotential η of 728 mV at a current density of ~2 mA cm^{-2} (TOF = 0.2 s^{-1}, Supporting Information). The catalytic wave was mostly retained in the presence of 0.25 mM Na_4EDTA, suggesting that catalytic activity is not due to Co(II), though it should be noted that $EDTA^{4-}$ is readily oxidized at E > 1.1 V vs NHE, which may account for slight differences in the shapes of the catalytic waves in the presence of Na_4EDTA.[36,37] Furthermore, rinsing the glassy carbon electrode with water removed all catalytic species that might have been on the electrode, as evidenced by the lack of catalysis in the cyclic voltammogram in a solution containing only electrolyte at pH 12 (Figure S1a). The electrocatalytic activity of **1** is also

DOI: 10.1021/jacs.5b08396
J. Am. Chem. Soc. 2015, 137, 12865−12872

Scheme 1. Observed Stoichiometric Intermediates Starting with 1

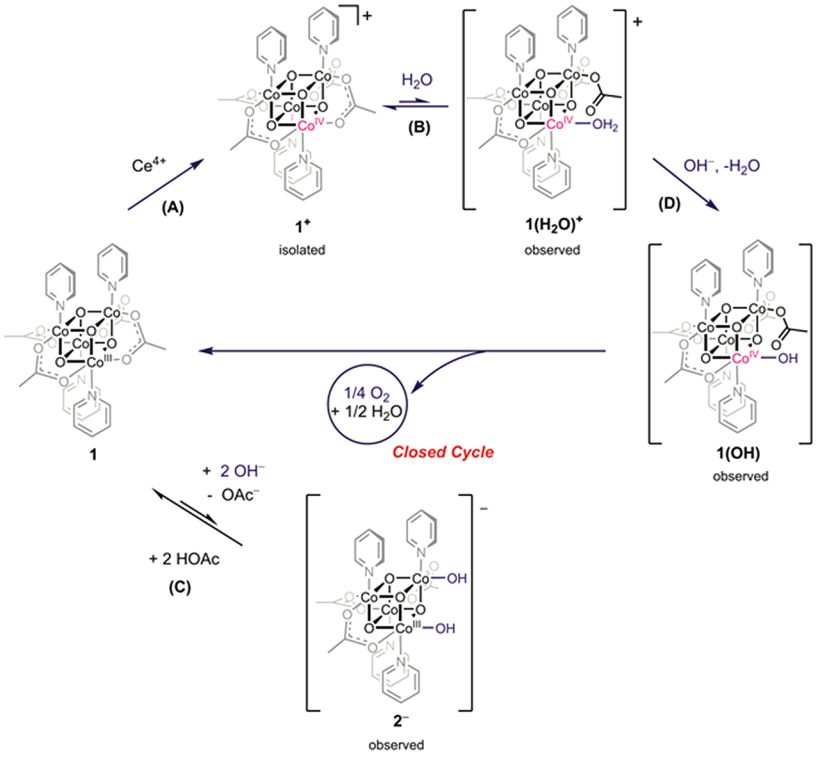

significantly different from that of Co(II) under these conditions (Figure S1a). From the CV and control experiments, it seems that very pure samples of **1** exhibit true homogeneous water oxidation catalysis at pH 12. To acquire a better understanding of the chemical behavior of complexes **1** and $\mathbf{1}^+$ at different pH values, attempts were made to isolate and/or observe the species responsible for the electrochemistry described above.

The pH-dependent behavior of **1** suggests that the protonated cubane, $\mathbf{1H}^+$, is present at lower pH values, and the existence of this complex was established by its isolation and characterization. Addition of 1 equiv of 4-toluenesulfonic acid (TsOH) to **1** in methanol afforded **[1H]OTs** in quantitative yield, and the structure of **[1H]OTs·4MeCN** was determined by X-ray crystallography (Figure S8a). With respect to **1**, the Co−OH bonds of **[1H]OTs** are elongated to an average length of 1.897(2) Å, while the remaining Co−O bond lengths remain unchanged with an average of 1.865(2) Å (**1** has a Co−O bond length range of 1.860−1.876 Å).[34] A close contact of 2.586(2) Å between an oxygen atom of the cubane (O(4)) and the tosylate oxygen atom O(13) is consistent with O···H···O hydrogen bonding. The ^{1}H NMR spectrum of **[1H]OTs** in CD_3CN at room temperature suggests that the molecule is C_s symmetric with broadened resonances, suggesting slow proton exchange on the NMR time scale. Furthermore, the infrared spectrum contains a broad peak at 3400 cm^{-1}, assigned to an O−H stretching mode.

The presence of a fully reversible redox couple over a wide pH range indicates that the chemical oxidation of **1** (or $\mathbf{1H}^+$) to $\mathbf{1}^+$ is feasible in water. Indeed, the oxidized cubane **[1]PF_6** has previously been isolated from the oxidation of **1** in acetonitrile.[29] In water, the reaction of **1** with 1 equiv of ceric ammonium nitrate, followed by addition of NH_4PF_6, resulted in precipitation of **[1]PF_6** as a black solid in 75% yield (Scheme 1, reaction A). Recrystallization from CH_2Cl_2/hexane afforded analytically pure single crystals of **[1]PF_6·CH_2Cl_2** for X-ray diffraction (XRD) analysis (Figure S8b). The Co−O bond distances in the cubane core of **[1]PF_6** are in agreement with those reported in the literature.[29,38]

The oxidized cubane **[1]PF_6** is soluble in a mixture of neutral water and acetonitrile (9:1 by volume), but appears to form an acidic aqua complex under these conditions. Thus, a decrease in the observed pH from 8.2 to 5.9 (with 0.4 mM **[1]PF_6**) is consistent with acidification of H_2O via coordination to cobalt, that is $\mathbf{1(H_2O)}^+ \rightleftharpoons \mathbf{1(OH)} + H^+$. The ^{1}H NMR spectrum of **[1]PF_6** in pure CD_3CN consists of four very broad resonances corresponding to equivalent acetate (10.17 ppm) and pyridine (6.62, 6.15, and 2.62 ppm) resonances. For a sample of **[1]PF_6** dissolved in 9:1 D_2O/CD_3CN, the same broad ^{1}H NMR resonances for **[1]PF_6** are observed, along with a set of four new resonances that correspond to a 23% conversion of **[1]PF_6** to a new species (Figure S4). The 8:8:4:12 ratio for these resonances is consistent with the presence of a new cubane species with four acetate and four pyridine ligands. The new resonances are paramagnetically shifted, as indicated by a pyridine-*H* chemical shift at 2.50 ppm, and an acetate-CH_3 resonance at 3.50 ppm. These results are consistent with the presence of a new Co(IV)-containing cubane cluster with an acidic aqua ligand, $\mathbf{1(H_2O)}^+$. Thus, an aqueous solution of **[1]PF_6** contains $\mathbf{1}^+$ and $\mathbf{1(H_2O)}^+$ in equilibrium, and the acidity of the latter species also implies the presence of **1(OH)** (Scheme 1, reaction B).

The species responsible for the anodic wave observed at pH 12 was targeted in the stoichiometric reaction of 1 equiv of NaOH with **1** in D_2O. By ^{1}H NMR spectroscopy, this reaction results in an equilibrium involving **1**, free acetate, and a new complex. Since many pyridine ligand resonances for the new complex overlap, ^{1}H TOCSY NMR spectroscopy was used to

DOI: 10.1021/jacs.5b08396
J. Am. Chem. Soc. 2015, 137, 12865−12872

resolve them, and the resulting assignments are consistent with a C_2-symmetric cubane complex possessing two types of pyridine ligands in a 1:1 ratio (Figure S5). Furthermore, two new acetate ligand resonances are present in a 6:3 ratio, and integration of the pyridine and acetate peaks shows that the new species possesses four pyridine and three acetate ligands. This is confirmed by ^{1}H pulsed field gradient spin−echo diffusion NMR spectroscopy, which shows that the new acetate and pyridine resonances belong to the same species having a hydrodynamic radius that is similar to that of **1** (r_H = 7.0 Å for **1**, and 6.8 Å for the new species). This information is most consistent with a [Co(III)$_4$]−dihydroxide complex, [Co_4O_4(OAc)$_3$py$_4$(OH)$_2$]$^-$ (**2**$^-$), formed by substitution of an acetate ligand by two hydroxide ions (Scheme 1, reaction C). The chemical identity of **2**$^-$ and the presence of hydroxide ligands was furthered evidenced by addition of 1 equiv of acetic acid to the reaction mixture, which reformed **1** in quantitative yield by ^{1}H NMR spectroscopy. Note that the structural *syn*-dihydroxide motif assigned to **2**$^-$ has been proposed in the literature as an active site for O_2 evolution in cobalt oxide materials.[17,30,31,39] Thus, an appealing mechanism for O_2 formation observed in the cyclic voltammogram involves electrochemical oxidation of **2**$^-$ to the [Co(III)$_3$Co(IV)]−dihydroxide state, followed by formation of the O−O bond. The possibility of a Co(IV) hydroxide complex as a catalyst for water oxidation prompted us to pursue the observation or isolation of such a species.

A conceivable pathway to a Co(IV) hydroxide complex in this system is by the associative addition of hydroxide to **1**$^+$. Interestingly, reaction of [**1**]**PF**$_6$ with 1 equiv of NaOH(aq) in CD_3CN quantitatively produced **1** (by ^{1}H NMR spectroscopy), indicating a net one-electron reduction of **1**$^+$ by hydroxide anion. On a larger scale, this reaction produced noticeable amounts of gas, suggesting the possibility of O_2 as a product of hydroxide oxidation by **1**$^+$. Quantitative measurement by an O_2-sensing probe revealed a ∼75% yield of O_2 with respect to **1**, though the yield is most likely higher since a nontrivial amount of unmeasured bubbles adhered to the wall of the flask (Figure 3A). Mass spectrometric measurement of the head space confirmed the presence of $^{32}O_2$, and when ∼97% enriched Na^{18}OH (in $H_2{}^{18}O$) was employed, 90% $^{36}O_2$ (94% theoretical) and 10% $^{34}O_2$ (5.9% theoretical) were detected (Figure 3B). High-resolution electrospray ionization mass spectrometry (ESI-MS) analysis of the solution after reaction with Na^{18}OH showed no measurable incorporation of ^{18}O into **1**, meaning that the O-atoms within the cluster do not exchange with OH^-/H_2O on the time scale of the experiment (Supporting Information). Significantly, this isotopic labeling experiment reveals that the O−O bond is formed solely from OH^- and *not* from the μ-O-atoms within the cuboidal core of **1**$^+$. Note that while oxygen isotopic labeling studies with a cobalt oxide (CoP_i) catalyst could not conclusively distinguish between mechanisms involving terminal versus bridging oxo/hydroxide ligands,[39] the results in this work favor mechanisms for which only terminal oxo/hydroxide ligands are involved in O−O bond formation. Furthermore, the reaction of **1**$^+$ with hydroxide supports the importance of the cobalt(IV) oxidation state in O_2 evolution by cobalt catalysts. The quantitative reduction of **1**$^+$ by hydroxide to regenerate **1** and give O_2 completes a conceivable catalytic cycle, for which each stoichiometric step of the cycle has been observed (Scheme 1, reaction D).

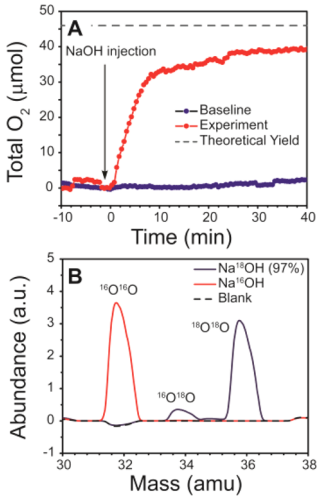

Figure 3. Measurement of O_2 from the reaction of [**1**]**PF**$_6$ and NaOH. (A) Quantification by fluorescence probe. (B) Isotopic quantification by mass spectrometry.

KINETICS AND PROPOSED MECHANISM

To gain further information on the mechanism of the reaction between [**1**]**PF**$_6$ and NaOH, a kinetics analysis of the reaction by stopped-flow UV−vis spectroscopy was conducted in 9:1 H_2O:MeCN. The reaction progress was monitored by decay of an absorption for [**1**]**PF**$_6$ at 280 nm. Two isosbestic points, at 335 and 362 nm, were observed for the reaction (Figure S6). These isosbestic points show that the decay of **1**$^+$ and growth of product **1** are nearly symmetrical with no measurable buildup of an intermediate. A striking feature of all kinetic experiments is the slightly sigmoidal decay of **1**$^+$ over the course of the reaction. The least-squares fit of the dependence of [**1**$^+$]$_0$ on the initial rate at 10 mM [OH^-] gives a mixed-order rate law containing a second-order term (k_{obs2} = 21 000 ± 4000 M^{-1} s^{-1}) and a first-order term (k_{obs1} = 0.8 ± 0.1 s^{-1}) (Figure 4A, eq 2).

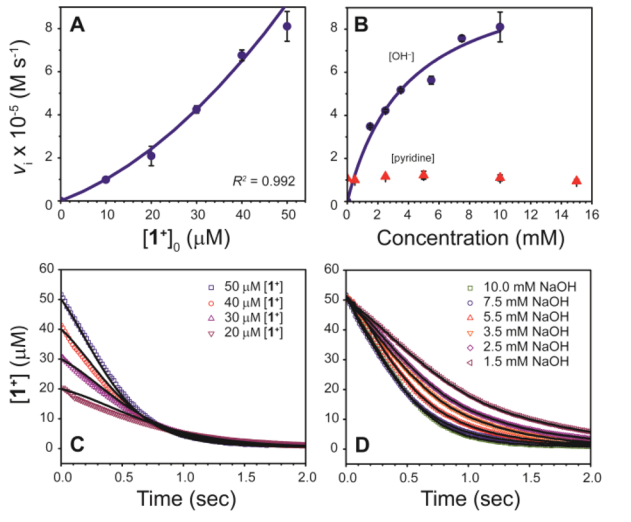

Figure 4. Kinetic plots. (A) Initial rate versus [**1**$^+$] (with 10 mM [OH^-]). (B) Initial rate versus [OH^-] (blue squares) and [pyridine] (with 5 mM [OH^-]) (red triangles). (C,D) Numerical kinetic modeling. The black solid lines are the fits from the model, and the points represent the measured values.

DOI: 10.1021/jacs.5b08396
J. Am. Chem. Soc. 2015, 137, 12865−12872

$$v_i = k_{obs1}[\mathbf{1}^+]_0 + k_{obs2}[\mathbf{1}^+]_0^2 \quad (2)$$

The second-order term strongly implicates the involvement of two molecules of $\mathbf{1}^+$ in the pathway to O−O bond formation, while the first-order term is consistent with either an activation of $\mathbf{1}^+$ or a concurrent pathway involving $\mathbf{1}^+$. Also, the rate of the reaction increased with increasing concentration of NaOH, but reached an asymptote at about 110 equiv of NaOH (6 mM, Figure 4B). This saturation behavior for NaOH suggests that OH^- reacts with an intermediate species whose concentration is limited. Four observations—the symmetry of growth and decay, the sigmoidal shape of the kinetic profile, the first- and second-order $[\mathbf{1}^+]$ terms in the rate law, and the saturation behavior of $[OH^-]$—are most consistent with a chain reaction propagated by a small amount of non-steady-state catalytic intermediate.[40] In this type of chain reaction mechanism, the reactant is both a pre-catalyst and a participant in a catalytic cycle. The precatalyst activation step gives rise to the first-order term, and the reaction of the precatalyst with a catalytic intermediate gives the second-order term. Saturation behavior in $[OH^-]$ is thus explained by reaction(s) of OH^- with catalytic intermediate(s). Pyridine has only a very weak inhibitory effect at high concentrations (16% rate decrease at 300 equiv of pyridine), implying that the reaction does not require dissociation of a pyridine ligand (Figure 4B). At 298 K, the activation free energy $\Delta G^{\ddagger}$ can be estimated from k_{obs2} to be 12 kcal/mol. When adjusted for the three steps involving H^+ transfer at pH 12 (−1.36ΔpH kcal/mol per deprotonation step) and a redox potential of 1.25 V (the redox potential for $\mathbf{1}/\mathbf{1}^+$), Siegbahn's calculated activation energy for O−O bond formation starting from Co(III) is 11.2 kcal/mol, which is very close to the value obtained from the kinetics.[30]

The proposed mechanism of Scheme 2 is consistent with all the experimental results described above. On the basis of the saturation behavior of hydroxide in this system, and the first-order term in the rate law (*vide supra*), catalyst generation likely results from formation of $\mathbf{1(OH)}$, by deprotonation of $\mathbf{1(H_2O)}^+$ or by addition of hydroxide ion to $\mathbf{1}^+$. The second-order term in $[\mathbf{1}^+]_0$ is explained by the participation of $\mathbf{1}^+$ as an oxidant in a proton-coupled electron transfer process with $\mathbf{1(OH)}$, represented in Scheme 2 by two steps (deprotonation followed by electron transfer) that generate the formally $[Co(III)_3Co(V)]$ species $\mathbf{1(O)}$. Note, however, that the order of deprotonation and electron transfer in the proposed mechanism is not distinguishable with these data. This unusually high oxidation state for cobalt is predicted to be favored over the $[Co(III)_2Co(IV)_2]$ state by several theoretical calculations; the oxidation state assignment is discussed in the following section.[30,32,33]

The reactions described above are consistent with the DFT calculations by Siegbahn for water oxidation, which indicate that $\mathbf{1(O)}^-$ is unable to engage in O−O bond formation by reaction with water; however, the higher oxidation state of $\mathbf{1(O)}$ should allow attack by water to produce the hydroperoxy species $\mathbf{1(OOH)}^-$.[30] Peroxide intermediates for cobalt catalysts have been speculated to exist based on observations by the groups of Frei and Stahl.[17,41] Finally, the OOH^- ligand may be readily oxidized to superoxide ($\mathbf{1(O_2^{\bullet})}^-$), then finally to O_2. The plausibility of the peroxide oxidation was tested by the reaction of $[\mathbf{1}]\mathbf{PF_6}$ with hydrogen peroxide, which gave O_2 and the reduced and protonated cubane, $[\mathbf{1H}]\mathbf{PF_6}$, characterized by ^{1}H NMR spectroscopy and single-crystal XRD (Figure S8). Kinetic measurements on the reaction in 9:1 MeCN:H_2O by stopped-flow UV−vis indicate clean first-order behavior for $[\mathbf{1}^+]$ and $[H_2O_2]$, with a second order rate constant of $k = 78 \pm 3\ M^{-1}\ s^{-1}$ at 25 °C. Replacement of $\mathbf{1(OH)}$ by $\mathbf{2}^-$ in the catalytic cycle should give the analogous intermediates, with the only difference being that an OAc^- ligand is replaced by an OH^- ligand.

Scheme 2. Proposed Mechanism for the Reduction of $\mathbf{1}^+$ to 1 by Hydroxide

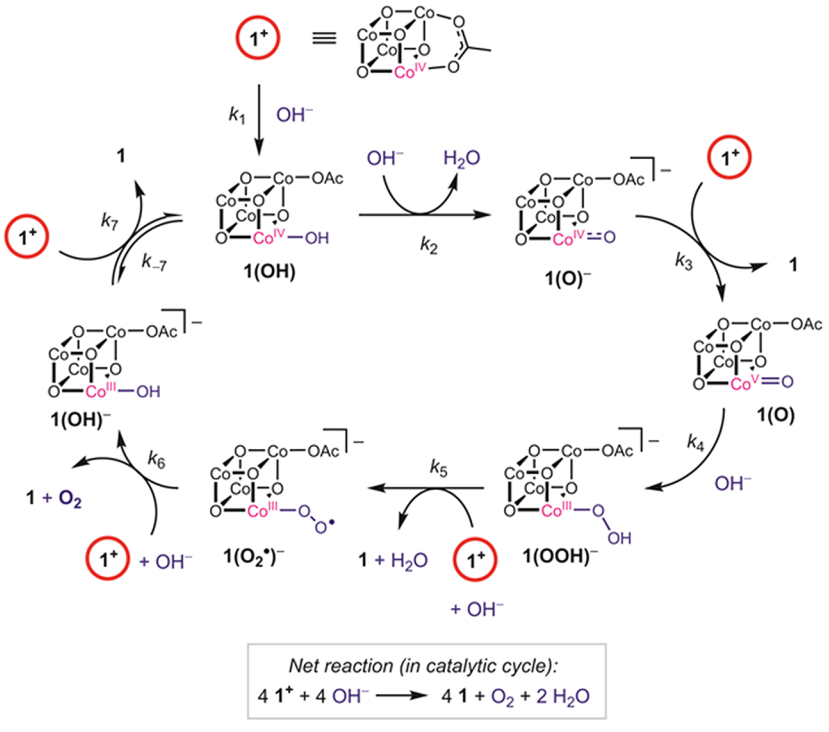

DOI: 10.1021/jacs.5b08396
J. Am. Chem. Soc. 2015, 137, 12865−12872

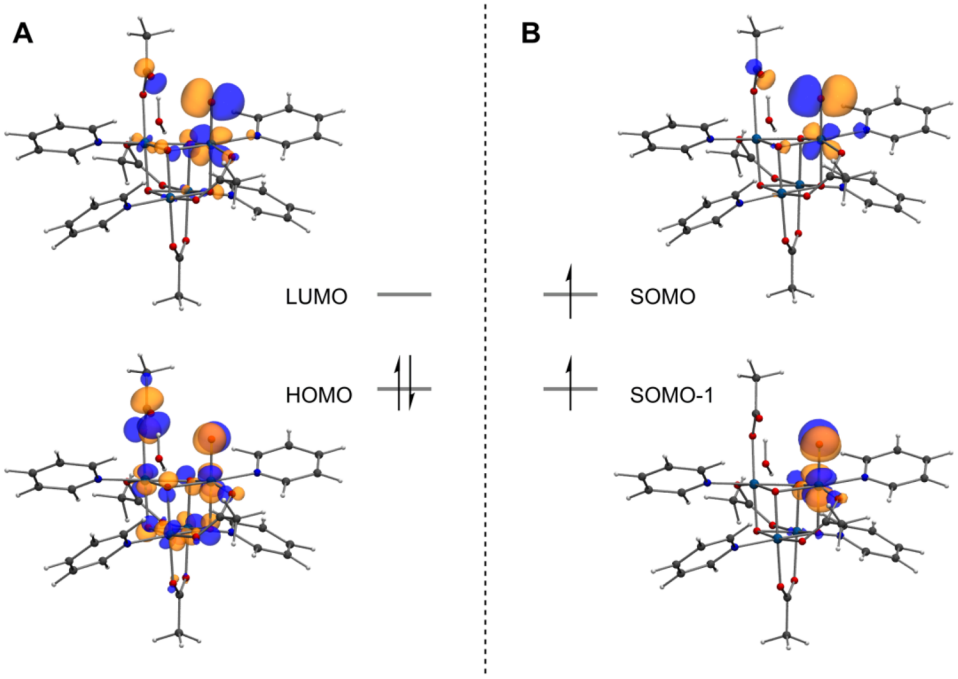

Figure 5. DFT-calculated molecular orbitals of **1(O)·H_2O** using B3LYP/6-31G+d,p: (a) singlet-state frontier orbitals and (b) triplet-state frontier orbitals (β-spin).

A possible related mechanism (Scheme S1) could involve displacement of acetate from **1(OH)** by hydroxide, to produce the dihydroxide **2**. This reaction would be analogous to that observed between **1** and OH^-, which leads to $\mathbf{2}^-$ and acetate (*vide supra*). The more oxidized dihydroxide **2**, with a $[Co(III)_3Co(IV)](OH)_2$ diamond core moiety, would then have to be oxidized (by $\mathbf{1}^+$) to a $[Co(III)_2Co(IV)_2]$ or $[Co(III)_3Co(V)]$ analogue before engaging in O−O bond formation across one face of the cubane. DFT calculations indicate that dicobalt centers like this may undergo O−O bond formation from the Co(IV)Co(IV) state, perhaps via deprotonation to an oxo−hydroxy intermediate.[31,42] Note that Siegbahn's DFT calculation indicates that a direct coupling mechanism of this type is less preferred in cubanes, by ∼3 kcal/mol.[30]

This complex mechanism was modeled numerically with global kinetics analysis, which successfully reproduced the initial rates, as well as the entire kinetic profile (Figure 4C,D). The model utilized eight rate constants (see Supporting Information); however, a sensitivity analysis revealed that only the values of k_1, k_3, and k_7 were major contributors for a good fit. Not surprisingly, those rate constants (k_1, k_3, and k_7) represent the key features of the mechanism: catalyst activation, oxidation to a formal Co(V) by disproportionation, and catalyst turnover. Similar conclusions about the rate equation could also be derived analytically, as follows. A rate law for the initial rates with excess $[OH^-]$ can be derived for the proposed mechanism using the steady-state approximation for all intermediates except **1(OH)** (see Supporting Information), which describes the experimental observations: the first- and second-order terms in $[\mathbf{1}^+]_0$, and the saturation behavior in $[OH^-]$ (eq 3).

$$-\frac{d[\mathbf{1}^+]}{dt} = k_1[\mathbf{1}^+][OH^-] + \frac{2k_2([\mathbf{1}^+]_0 - [\mathbf{1}^+] - [\mathbf{1}])[OH^-]}{k_2\frac{[OH^-]}{[\mathbf{1}^+]}\left(\frac{k_3+k_7}{k_3k_7}\right) + \frac{k_2}{k_4} + \frac{k_2}{k_5[\mathbf{1}^+]} + \frac{k_2}{k_6[\mathbf{1}^+]} + \frac{k_{-7}[\mathbf{1}]}{k_7[\mathbf{1}^+]} + 1} \quad (3)$$

At very high concentrations of $[OH^-]$, low concentrations of product ($[\mathbf{1}] \approx 0$), and for $[\mathbf{1}^+] = f[\mathbf{1}^+]_0$ (where $0 < f < 1$), the rate law reduces to eq 2, with the expressions for k_{obs1} and k_{obs2} given in eqs 4 and 5.

$$k_{obs1} = k_1 f[OH^-] \quad (4)$$

$$k_{obs2} = \frac{2k_3k_7}{k_3 + k_7}(f - f^2) \quad (5)$$

Again, it is shown that the kinetics (under excess $[OH^-]$ conditions) depend only on k_1, k_3, and k_7, in good agreement with the numerical fitting. Additionally, it can be shown that the exact expression of $[\mathbf{1}^+](t)$ over *all time* is a sigmoidal curve (eq S12 and Figure S7). The consistency of this model with all the observations is compelling evidence for the proposed mechanism.

NATURE OF THE HIGHLY OXIDIZED INTERMEDIATE

The kinetic experiments discussed above suggest that the formal $[Co(III)_3Co(IV)]$ oxidation state disproportionates into the $[Co(III)_4]$ state and a higher oxidation state, $[Co(III)_2Co(IV)_2]$ or $[Co(III)_3Co(V)]$. Of course, the concept of oxidation state is merely a formalism having a defined set of rules,[43] and extrapolation of this formalism to actual charge distributions must be made with caution. Nonetheless, it may be instructive to determine the location of the electron hole in the oxidized cluster. Significantly, Co(V) has never been observed spectroscopically but it has often been suggested by

DOI: 10.1021/jacs.5b08396
J. Am. Chem. Soc. 2015, 137, 12865−12872

calculations. If the mechanism suggested by the kinetic data is correct, it would not be possible to build up significant concentrations of the formal $[Co(III)_3Co(V)]$ species $\mathbf{1(O)}$ for typical spectroscopic investigations. Therefore, we chose to investigate the nature of this intermediate species with DFT calculations.

First, the feasibility of the Co(V) oxidation state may be considered on the basis of simple ligand-field arguments. While it has been demonstrated that the electron hole in the $[Co(III)_3Co(IV)]$ complex ($\mathbf{1}^+$) is completely delocalized over the cubane (each Co is better described with an "oxidation state"/charge of +3.125),[25] introduction of the strongly π-basic terminal oxo ligand at one cobalt center in the cubane ($\mathbf{1(O)}^-$) is expected to raise the energy of the corresponding t_{2g}-like orbitals to effectively localize the electron hole at that particular cobalt ion. Stated another way, the electron hole should be most stable on the cobalt ion associated with the π-basic terminal oxo ligand. Thus, the terminal oxo ligand should cause a shift from $[Co(+3.125)_4]$ toward $[Co(III)_3Co(IV)]$. By the same argument, the $[Co(III)_3Co(V)]$ state should also be a better description than $[Co(III)_2Co(IV)_2]$ in the $\mathbf{1(O)}$ complex, as the presence of the terminal oxo ligand should also cause preferential localization of the hole. These ligand-field rationalizations provide an intuitive albeit rough guide for possible oxidation state assignments.

DFT can potentially provide a more quantitative description of the oxidation state. Complex $\mathbf{1(O)}$ has been described by Siegbahn[30] to have an $S = 1$ ground state, with an $S = 0$ excited state 5.6 kcal/mol higher in energy. Inspection of the molecular orbitals in both the triplet and singlet states indicates significant localization of the SOMO and LUMO, respectively, on the terminal Co−oxo moiety (Figure 5). In the triplet state, the β-spin wave functions reside predominately on the Co−O unit, while the α-electron wave functions are more delocalized throughout the cubane. Similarly, in the singlet state, the LUMO is localized on the Co−O unit. These results reiterate the spin-density calculations by Siegbahn, and are also more consistent with the formal $[Co(III)_3Co(V)]$ oxidation state. In summary, both ligand-field arguments and DFT calculations support the formal oxidation state in $\mathbf{1(O)}$ as being described as $[Co(III)_3Co(V)]$ rather than $[Co(III)_2Co(IV)_2]$.

CONCLUSIONS

The characterization of species implicated by electrochemical experiments over a wide pH range provides important insights into the reactivity of a cobalt cubane cluster. The $[Co(III)_4]$ cubane **1** reacts with H^+ as well as OH^- to give observable products. Although it is difficult to establish the identity of the electrocatalyst implicated by CV studies, stoichiometric reactivity demonstrates that cobalt cubane **1** reacts with OH^- to produce a likely WOC, and the $[Co(III)_3Co(IV)]$ cubane ($[\mathbf{1}]\mathbf{PF_6}$) reacts with OH^- to produce O_2 with quantitative reduction to **1**. These reactions strongly suggest that there exists at least one molecular, homogeneous pathway for O_2 evolution by cobalt cubane complexes. Kinetic experiments on the stoichiometric oxygen evolution from $\mathbf{1}^+$ provide strong, direct evidence for the homogeneous nature of the reaction, especially as it obeys a rate law consistent with the proposed mechanism. The second-order term in $[\mathbf{1}^+]$ indicates that a more oxidized state for the cubane, formally $[Co(III)_3Co(V)]$, must be reached via disproportionation of the $[Co(III)_3Co(IV)]$ state, before O_2 evolution. The participation of a terminal cobalt−oxo intermediate is supported by several observations, including the non-involvement of cubane oxo ligands in the formation of O_2, the viability of intermediates $\mathbf{1(H_2O)}^+$ and $\mathbf{1(OH)}$, and the dependence of the rate on $[OH^-]$. Furthermore, the experimentally determined activation energy is consistent with theoretical values reported in the literature. This study helps solidify the role of cobalt cubane complexes as WOCs, and as useful structural and functional models for cobalt oxide materials. Significantly, this work suggests that O−O bond formation on cobalt oxide occurs via terminal oxo, rather than bridging oxo ligands present at edge sites.

These results provide several guidelines relevant to future catalyst design strategies. The most relevant formal oxidation states for cobalt WOCs appear to be +3, + 4, and +5, while the +2 oxidation state does not appear to be necessary in the catalytic cycle. Thus, supporting frameworks should be designed to stabilize the higher oxidation states such as Co(IV) and Co(V). Multimetallic oxido systems, such as the cobalt cubane described herein, are well suited to stabilize such states, as they can relieve the burden of an unstable oxidation state by sharing an electron hole throughout the cluster. Ancillary ligands may play a key role in tuning a cluster's redox potentials to those appropriate for efficient water oxidation. In addition, catalyst design must allow for water or hydroxide to bind to the cobalt center, as this is the first step toward generating the putative high-valent cobalt−oxo intermediate. Finally, since bridging oxo ligands do not appear to play a direct role in O_2 formation, design elements that allow formation of terminal cobalt−oxo moieties, while stabilizing the $[Co_4O_4]$ core, may prove advantageous to water oxidation catalysis.

ASSOCIATED CONTENT

Supporting Information

The Supporting Information is available free of charge on the ACS Publications website at DOI: 10.1021/jacs.5b08396. CIF files can also be obtained free of charge from the Cambridge Crystallographic Data Centre under reference numbers CCDC-1054644, CCDC-1054645, and CCDC-1054646.

Full experimental details and spectroscopic data (PDF)
X-ray crystallographic data for $[\mathbf{1H}]\mathbf{PF_6}\cdot\mathbf{2H_2O}$ (CIF)
X-ray crystallographic data for $[\mathbf{1}]\mathbf{PF_6}$ (CIF)
X-ray crystallographic data for $[\mathbf{1H}]\mathbf{OTs}$ (CIF)

AUTHOR INFORMATION

Corresponding Author

*tdtilley@berkeley.edu

Notes

The authors declare no competing financial interest.

ACKNOWLEDGMENTS

We thank Heinz Frei for help with the mass spectrometry measurements of O_2, Anthony T. Iavarone for ESI-MS (QB3 Chemistry Mass Spectrometry Facility), and Kurt van Allsburg, Gavin R. Kiel, Patrick W. Smith, Robert G. Bergman, and Richard G. Finke for helpful discussions. We also thank Antonio DiPasquale for assistance with solving X-ray diffraction structures, and the NIH Shared Instrumentation Grant S10-RR027172. This work was supported by the Director, Office of Science, Office of Basic Energy Sciences of the U.S. Department of Energy under contract no. DE-AC02-05CH11231. P.O.-B. acknowledges grant PIOF-GA-2011-299571 (7th FP, People Marie Curie Actions) for funding.

DOI: 10.1021/jacs.5b08396
J. Am. Chem. Soc. 2015, 137, 12865−12872

REFERENCES

(1) *Climate Change 2014: Synthesis Report*; Contribution of Working Groups I, II, and III to the Fifth Assessment Report of the Intergovernmental Panel on Climate Change; Core Writing Team, Pachauri, R. K., Meyer, L., Eds.; IPCC: Geneva, Switzerland, 2014; p 138.
(2) Lewis, N. S.; Nocera, D. G. *Proc. Natl. Acad. Sci. U. S. A.* **2006**, *103*, 15729−15735.
(3) Barber, J. *Chem. Soc. Rev.* **2009**, *38*, 185−196.
(4) Moore, G. F.; Brudvig, G. W. *Annu. Rev. Condens. Matter Phys.* **2011**, *2*, 303−327.
(5) Eisenberg, R.; Gray, H. B. *Inorg. Chem.* **2008**, *47*, 1697−1699.
(6) Rüttinger, W.; Dismukes, G. C. *Chem. Rev.* **1997**, *97*, 1−24.
(7) Walter, M. G.; Warren, E. L.; McKone, J. R.; Boettcher, S. W.; Mi, Q.; Santori, E. A.; Lewis, N. S. *Chem. Rev.* **2010**, *110*, 6446−6473.
(8) Kärkäs, M. D.; Verho, O.; Johnston, E. V.; Åkermark, B. *Chem. Rev.* **2014**, *114*, 11863−12001.
(9) Cox, N.; Retegan, M.; Neese, F.; Pantazis, D. A.; Boussac, A.; Lubitz, W. *Science* **2014**, *345*, 804−808.
(10) Kern, J.; Alonso-Mori, R.; Tran, R.; Hattne, J.; Gildea, R. J.; Echols, N.; Glöckner, C.; Hellmich, J.; Laksmono, H.; Sierra, R. G.; Lassalle-Kaiser, B.; Koroidov, S.; Lampe, A.; Han, G.; Gul, S.; DiFiore, D.; Milathianaki, D.; Fry, A. R.; Miahnahri, A.; Schafer, D. W.; Messerschmidt, M.; Seibert, M. M.; Koglin, J. E.; Sokaras, D.; Weng, T.-C.; Sellberg, J.; Latimer, M. J.; Grosse-Kunstleve, R. W.; Zwart, P. H.; White, W. E.; Glatzel, P.; Adams, P. D.; Bogan, M. J.; Williams, G. J.; Boutet, S.; Messinger, J.; Zouni, A.; Sauter, N. K.; Yachandra, V. K.; Bergmann, U.; Yano, J. *Science* **2013**, *340*, 491−495.
(11) Betley, T. A.; Wu, Q.; Van Voorhis, T.; Nocera, D. G. *Inorg. Chem.* **2008**, *47*, 1849−1861.
(12) Delaplane, R. G.; Ibers, J. A.; Ferraro, J. R.; Rush, J. J. *J. Chem. Phys.* **1969**, *50*, 1920−1927.
(13) Kanan, M. W.; Nocera, D. G. *Science* **2008**, *321*, 1072−1075.
(14) Jiao, F.; Frei, H. *Angew. Chem., Int. Ed.* **2009**, *48*, 1841−1844.
(15) Esswein, A. J.; McMurdo, M. J.; Ross, P. N.; Bell, A. T.; Tilley, T. D. *J. Phys. Chem. C* **2009**, *113*, 15068−15072.
(16) Hans Wedepohl, K. *Geochim. Cosmochim. Acta* **1995**, *59*, 1217−1232.
(17) Zhang, M.; de Respinis, M.; Frei, H. *Nat. Chem.* **2014**, *6*, 362−367.
(18) Ahn, H. S.; Yano, J.; Tilley, T. D. *Energy Environ. Sci.* **2013**, *6*, 3080−3087.
(19) Yin, Q.; Tan, J. M.; Besson, C.; Geletii, Y. V.; Musaev, D. G.; Kuznetsov, A. E.; Luo, Z.; Hardcastle, K. I.; Hill, C. L. *Science* **2010**, *328*, 342−345.
(20) Wasylenko, D. J.; Ganesamoorthy, C.; Borau-Garcia, J.; Berlinguette, C. P. *Chem. Commun.* **2011**, *47*, 4249−4251.
(21) Wang, D.; Groves, J. T. *Proc. Natl. Acad. Sci. U. S. A.* **2013**, *110*, 15579.
(22) Stracke, J. J.; Finke, R. G. *ACS Catal.* **2014**, *4*, 909−933.
(23) Stracke, J. J.; Finke, R. G. *J. Am. Chem. Soc.* **2011**, *133*, 14872−14875.
(24) Beattie, J. K.; Hambley, T. W.; Klepetko, J. A.; Masters, A. F.; Turner, P. *Polyhedron* **1998**, *17*, 1343−1354.
(25) McAlpin, J. G.; Stich, T. A.; Ohlin, C. A.; Surendranath, Y.; Nocera, D. G.; Casey, W. H.; Britt, R. D. *J. Am. Chem. Soc.* **2011**, *133*, 15444−15452.
(26) McCool, N. S.; Robinson, D. M.; Sheats, J. E.; Dismukes, G. C. *J. Am. Chem. Soc.* **2011**, *133*, 11446−11449.
(27) La Ganga, G.; Puntoriero, F.; Campagna, S.; Bazzan, I.; Berardi, S.; Bonchio, M.; Sartorel, A.; Natali, M.; Scandola, F. *Faraday Discuss.* **2012**, *155*, 177−190.
(28) Zhang, B.; Li, F.; Yu, F.; Wang, X.; Zhou, X.; Li, H.; Jiang, Y.; Sun, L. *ACS Catal.* **2014**, *4*, 804−809.
(29) Ullman, A. M.; Liu, Y.; Huynh, M.; Bediako, D. K.; Wang, H.; Anderson, B. L.; Powers, D. C.; Breen, J. J.; Abruña, H. D.; Nocera, D. G. *J. Am. Chem. Soc.* **2014**, *136*, 17681−17688.
(30) Li, X.; Siegbahn, P. E. M. *J. Am. Chem. Soc.* **2013**, *135*, 13804−13813.
(31) Wang, L.-P.; Van Voorhis, T. *J. Phys. Chem. Lett.* **2011**, *2*, 2200−2204.
(32) Fernando, A.; Aikens, C. M. *J. Phys. Chem. C* **2015**, *119*, 11072−11085.
(33) Mattioli, G.; Giannozzi, P.; Amore Bonapasta, A.; Guidoni, L. *J. Am. Chem. Soc.* **2013**, *135*, 15353−15363.
(34) Chakrabarty, R.; Bora, S. J.; Das, B. K. *Inorg. Chem.* **2007**, *46*, 9450−9462.
(35) Symes, M. D.; Surendranath, Y.; Lutterman, D. A.; Nocera, D. G. *J. Am. Chem. Soc.* **2011**, *133*, 5174−5177.
(36) Pakalapati, S. N. R.; Popov, B. N.; White, R. E. *J. Electrochem. Soc.* **1996**, *143*, 1636−1643.
(37) Eckenhoff, W. T.; Eisenberg, R. *Dalton Trans.* **2012**, *41*, 13004.
(38) Stich, T. A.; Krzystek, J.; Mercado, B. Q.; McAlpin, J. G.; Ohlin, C. A.; Olmstead, M. M.; Casey, W. H.; David Britt, R. *Polyhedron* **2013**, *64*, 304−307.
(39) Surendranath, Y.; Kanan, M. W.; Nocera, D. G. *J. Am. Chem. Soc.* **2010**, *132*, 16501−16509.
(40) Mower, M. P.; Blackmond, D. G. *J. Am. Chem. Soc.* **2015**, *137*, 2386−2391.
(41) Gerken, J. B.; McAlpin, J. G.; Chen, J. Y. C.; Rigsby, M. L.; Casey, W. H.; Britt, R. D.; Stahl, S. S. *J. Am. Chem. Soc.* **2011**, *133*, 14431−14442.
(42) Davenport, T. C.; Ahn, H. S.; Ziegler, M. S.; Tilley, T. D. *Chem. Commun.* **2014**, *50*, 6326−6329.
(43) IUPAC. *Compendium of Chemical Terminology*, 2nd ed. (the "Gold Book"); McNaught, A. D., Wilkinson, A., Compilers; Blackwell Scientific Publications: Oxford, 1997.

DOI: 10.1021/jacs.5b08396
J. Am. Chem. Soc. 2015, 137, 12865−12872